Reconstructing the annual mass balance of glaciar Echaurren Norte (Central Andes, 33.5°S) using local and regional hydro-climatic data

M.H. Masiokas[1]*, D.A. Christie[2,3], C. Le Quesne[2], P. Pitte[1], L. Ruiz[1], R. Villalba[1], B.H. Luckman[4], E. Berthier[5], S.U. Nussbaumer[6], A. González-Reyes[7], J. McPhee[8], G. Barcaza[9]

[1] Instituto Argentino de Nivología, Glaciología y Ciencias Ambientales (IANIGLA), CCT- CONICET Mendoza, C.C. 330, (5500) Mendoza, Argentina

[2] Laboratorio de Dendrocronología y Cambio Global, Instituto de Conservación Biodiversidad y Territorio, Facultad de Ciencias Forestales y Recursos Naturales, Universidad Austral de Chile, Valdivia, Chile.

[3] Center for Climate and Resilience Research (CR)[2], Chile.

[4] Department of Geography, University of Western Ontario, Canada.

[5] LEGOS, CNRS, Université de Toulouse, France

[6] Department of Geography, University of Zurich, and Department of Geosciences, University of Fribourg, Switzerland.

[7] Departamento de Geología, Facultad de Ciencias Físicas y Matemáticas, Universidad de Chile.

[8] Departamento de Ingeniería Civil, Facultad de Ciencias Físicas y Matemáticas, Universidad de Chile.

[9] Dirección General de Aguas (DGA), Santiago, Chile.

* Correspondence to: mmasiokas@mendoza-conicet.gob.ar

Tel.: +54-261-5244264

Fax: +54-261-5244201

Abstract

Despite the great number and variety of glaciers in southern South America, *in situ* glacier mass balance records are extremely scarce and glacier-climate relationships are still poorly understood in this region. Here we use the longest (>35 yrs) and most complete *in situ* mass balance record, available for glaciar Echaurren Norte in the Andes at ~33.5°S, to develop a minimal glacier surface mass balance model that relies on nearby monthly precipitation and air temperature data as forcing. This basic model is able to explain 78% of the variance in the annual glacier mass balance record over the 1978-2013 calibration period. An attribution assessment identified precipitation variability as the dominant forcing modulating annual mass balances at ECH, with temperature variations likely playing a secondary role. A regionally-averaged series of mean annual streamflow records from both sides of the Andes between ~30° and 37°S is then used to estimate, through simple linear regression, this glacier's annual mass balance variations since 1909. The reconstruction model captures 68% of the observed glacier mass balance variability and shows three periods of sustained positive mass balances embedded in an overall negative trend over the past 105 years. The three periods of sustained positive mass balances (centered in the 1920s-30s, in the 1980s and in the first decade of the 21st century) coincide with several documented glacier advances in this region. Similar trends observed in other shorter glacier mass balance series suggest that the glaciar Echaurren Norte reconstruction is representative of larger-scale conditions and could be useful for more detailed glaciological, hydrological and climatological assessments in this portion of the Andes.

1. Introduction

The extra-tropical Andes between ~23° and 55°S contain a large number and variety of glaciers ranging from small glacierets at elevations of over 6000 m in the high, arid Andes of northern Chile and Argentina, to large outlet glaciers that reach the sea in the humid southwestern portion of Patagonia and Tierra del Fuego. Altogether, these ice masses concentrate the largest glacierized area in the Southern Hemisphere outside Antarctica and are highly valued as sources of freshwater, as indicators of climatic change, as tourist attractions, and as environmental and cultural icons in different sectors of the Andes. As reported for other mountainous areas of the globe, glaciers in southern South America display a widespread retreating pattern that has been usually attributed to warmer, and sometimes drier, climatic conditions in this region (Villalba et al. 2003; Rignot et al. 2003; Rivera et al. 2000, 2005; Masiokas et al. 2008, 2009; Le Quesne et al. 2009; Pellicciotti et al. 2014). Quantitative assessments of regional glacier mass balance changes and glacier-climate relationships are, however, seriously hampered by the scarcity and short length of *in situ* glacier mass balance data and proximal climate records within the Andes. The latest publication of the World Glacier Monitoring Service (WGMS 2013) reports annual mass balance measurements for seven extratropical Andean glaciers (five in Argentina, two in Chile). Four of these records start in 2010 and are for small glaciers and glacierets located ca. 29.30°S, two records are located between 32°-34°S and start in the mid-late 1970s, and the remaining record from Tierra del Fuego (54.8°S) starts in 2001. Discontinued, short-term glacier mass balance measurements (see e.g. Popovnin et al. 1999) and recent programs initiated at new sites (e.g. Rivera et al. 2005; Rabatel et al. 2011; Ruiz et al. 2013) complete the network of direct glacier mass balance data currently available in southern South America. Although not optimal in terms of spatial coverage, arguably the single most important limitation of this network is the short period of time covered by consistent, reliable records. Of the two longest mass balance series mentioned above (glaciar Echaurren Norte and glaciar Piloto Este in the Central Andes, see Table 1.1 in WGMS 2013), only the series from Echaurren Norte in Chile (Fig. 1A-C) provides a complete record spanning more than 35 years. In fact, this series constitutes the longest direct glacier mass balance record in the Southern Hemisphere (see Escobar et al. 1995a,b; DGA 2010 and WGMS 2013) and is thus a “reference” glacier in the WGMS global assessments. The mass balance record from glaciar Piloto Este (located ca. 100 km to the north in Argentina; Fig. 1A) covers the 1979-2002 period and contains several data gaps that have been interpolated using various techniques (Leiva et al. 2007).

Many studies dealing with recent climate and glacier changes in southern South America have pointed out the shortness, poor quality, or absence of climatic records at high elevation sites or in the proximity of glaciers in the Andes (Villalba et al. 2003; Rivera et al. 2005; Masiokas et al. 2008; Rasmussen et al. 2007; Falvey and Garreaud 2009; Pellicciotti et al. 2014; Vuillle et al. 2015). Given the lack of suitable data, many climatic assessments have used records from distant, low elevation weather stations and/or gridded datasets to estimate conditions and recent climate variability within the Andean range. It is interesting to note, however, that the amount of hydro-climatic information (in particular from solid and liquid precipitation, and hydrologic variables) is comparatively better for those portions of the southern Andes that support large populated centers and where the water provided by the mountains is vital for human consumption, agriculture, industries and/or hydropower generation. In these areas, mainly between ca. 29° and 42°S, local and national water resource agencies have monitored a well-maintained network of hydrologic and meteorological stations for several decades (see e.g. Masiokas et al. 2006, 2010). The data from the stations in this region are slowly becoming publicly available and are substantially better in terms of quantity and quality than those for the less populated, more inaccessible areas in southern Patagonia or in the Desert Andes of northern Chile and Argentina.

The Central Andes of Chile and Argentina between ~31° and 35°S (see Lliboutry 1998) have a mean elevation of about 3500 m with several peaks reaching over 6000 m (Fig. 1A). The climate of this region is characterized by a Mediterranean regime with a marked precipitation peak during the cold months (April to October) and little precipitation during the warm summer season (November to March; Fig. 1D). Almost all of the moisture comes from westerly Pacific frontal systems, precipitating as rainfall in the Chilean lowlands and as snow in the Andes to the east (Miller 1976; Aceituno 1988; Garreaud 2009). The snow accumulated in the mountains during winter remains frozen until the onset of the melt season (usually October-November), producing a unimodal snowmelt-dominated regime for all rivers originating on either side of the Andes at these latitudes (Masiokas et al. 2006; Cara et al. in press). This relatively simple configuration entails some potential benefits for the study and understanding of the hydro-climatic and glaciological processes in this region: First, the strong co-variability between total rainfall amounts measured in central Chile and winter snow accumulation and river discharges recorded in the Andes (see Fig. 2) allows the use of a relatively limited number of station records to capture the main regional hydro-climatic patterns. The strong common signal among these variables also offers the possibility of inferring or reconstructing selected instrumental data (e.g. winter snow accumulation, which begins in 1951) using data from other well-correlated variables with a longer temporal coverage (e.g. Andean streamflow records which are available since 1909). Masiokas et al. (2012) used these relationships to extend Andean snowpack variations using central Chile rainfall records and precipitation-sensitive tree-ring width series.

In contrast to the well-known similarities between precipitation (solid and liquid) and surface runoff, the spatial and temporal patterns of high-elevation temperature records in the Central Andes of Chile and Argentina are still poorly understood. Falvey and Garreaud (2009) presented a detailed assessment of temperature trends over the 1979-2006 period along the western margin of subtropical South America, reporting a notable contrast between surface cooling (-0.2°C/decade) in coastal stations and a warming trend of ca. +0.25°C/decade in the Andes only 100-200 km inland. However, only two land stations were available with long enough records above 2000 m (i.e. El Yeso and Lagunitas stations in Chile at 2475 and 2765 m, respectively), but radiosonde data from the coastal station Quintero (ca. 33°S) showed comparable positive trends for the free-troposphere (Falvey and Garreaud 2009). This lack of high elevation surface temperature data also restricted the recent assessments of Vuille et al. (2015), who focused their elevation-dependent temperature trend analyses on the region north of 18°S because data were too sparse farther south.

The station El Yeso (33°40’36”S, 70°05’19”W) is located only 10 km south of glaciar Echaurren Norte (Fig. 1B). Mean daily and monthly temperature and total precipitation measurements from this station are available since 1962 but contain several months with missing data prior to 1977 (temperature) and 1975 (precipitation). Since 1977, both series are practically complete and updated on a regular basis. To our knowledge, in the entire extra-tropical Andes there is no other operational meteorological station with such a long and complete record of temperature and precipitation variations less than a few kilometres from a glacier, which moreover contains the longest ongoing mass balance monitoring program in the Southern Hemisphere. This rare combination of relatively long, complete climate records near a well-studied glacier site clearly highlights the importance of this unique location for varied glaciological and climatological investigations in the southern Andes.

In this contribution we use seasonal mass balance records from glaciar Echaurren Norte plus local and regionally-averaged monthly hydro-climatic data to model and reconstruct annual glacier mass balance changes over the past 105 years. Since only the glacier-wide seasonal and annual mass balance components are available for ECH, one of the main objectives of the study was to explore the suitability of simple mass balance models that require a minimum amount of input data (Marzeion et al. 2012; see also Kaser et al. 2010). Although this simplistic approach provides limited insight into the intricate physical processes involved in this glacier's intra-annual mass balance variations, it may, nonetheless, offer a useful starting point to address some basic (yet still poorly known) questions regarding the glacier's sensitivity to climate variations. We did not consider a data-intensive approach to measure and model the complex daily energy and mass balance variations of this glacier (e.g. Pellicciotti et al. 2014) because of the lack of the high resolution, *in situ* meteorological and glaciological measurements usually required in these type of analyses. Another primary objective was to use the available, well correlated hydrological records from this region (Fig. 2) to extend the ECH annual mass balance record and evaluate the fluctuations of mass balance over a much longer period than that covered by regular glaciological measurements. Comparisons with other shorter mass balance series and with a record of glacier advances in this region suggest the resulting time series contain a discernible regional footprint. Overall, we believe the findings discussed below constitute a substantial improvement in the understanding of the main patterns and forcings of the glacier mass balance changes in this region and provide a useful background for more detailed glacio-climatic assessments and modeling exercises in this portion of the Andes.

2 – Data and Methods

2.1. Glacier mass balance data

Glaciar Echaurren Norte (33°33'S, 70°08'W; hereafter ECH) is located within a southwestern oriented cirque ~50 km southeast of Santiago de Chile, in the headwaters of the Maipo river basin

(Fig. 1A-C). ECH provides water to Laguna Negra, a natural lake that together with the nearby El Yeso artificial lake constitute crucial water reservoirs for extensive irrigated lands and for the metropolitan Santiago area in Central Chile.

Mass balance measurements started at this easily accessible glacier in the austral spring of 1975 under the auspices of Dirección General de Aguas (DGA), the institution in charge of monitoring and managing water resources in Chile. Summer and winter mass balance data at ECH have been regularly measured until the present by DGA officials, and have been reported in sporadic internal documents and scientific publications (Peña and Narbona 1978; Peña et al. 1995; Escobar et al. 1995, 1997; DGA 2010). These records have also been reported to the WGMS, from where we obtained the 1975-2012 data used in this manuscript (annual mass balance data extend to 2013; see WGMS 2013 and www.wgms.ch). The glacier has thinned in the last decades and presently consists of small remnants of both clean and debris-covered ice (Fig. 1C). Despite this evident ice mass loss, the elevation range of the glacier has not changed much since measurements started in the mid 1970s. According to Peña and Narbona (1978) and Escobar et al. (1995), in the first years of the mass balance program the glacier covered an area of 0.4 km^2 distributed over a short elevation range between ca. 3650 and 3880 m asl (Fig. 1C). Over the time period covered by the mass balance records, no adjustment has been made to incorporate the changes in surface area of the glacier, and thus the reported values are considered here as reference-surface mass balance estimates (i.e. the mass balance that would have been observed if the glacier topography had not changed over the study period; see Cogley et al. 2011).

Mass balance data from glaciar Piloto Este (hereafter PIL) from 1979-2002 and shorter time series from small glaciers and glacierets further north in this region are also available from the WGMS database (Leiva et al. 2007; Rabatel et al. 2011; WGMS 2013; see Fig. 1A and Table 1). Here we compare the cumulative annual mass balance records of these glaciers as independent validation measures of the main patterns and temporal trends observed in the measured and modeled mass balance series from ECH.

2.2 Minimal glacier mass balance model

A minimal model only requiring monthly temperature and precipitation data (Marzeion et al. 2012) was used to estimate the interannual surface mass balance variations of ECH and to explore the relative importance of temperature and precipitation variability on the ECH records. In their publication, Marzeion et al. (2012) used gridded precipitation and temperature data to calibrate individual models for 15 glaciers with existing mass balance measurements in the greater Alpine region. The climate data used here come from El Yeso, a permanent automatic weather station maintained by DGA and located ca. 10 km to the south and 1200 m lower than ECH's snout (Fig. 1B). The data are freely available at the DGA website (www.dga.cl) and contain practically complete monthly temperature and precipitation records since 1977 (only four missing months were filled using their long-term means). The mass balance model can be defined as follows:

$$MB = \sum_{i=1}^{12} (\alpha P_i - \mu(\max(0, T_i - T_{melt}))) \quad (1)$$

where MB represents the modeled annual specific mass balance of the glacier, P_i are monthly total precipitation values at the El Yeso station, and α is a scaling parameter introduced to compensate for the precipitation gradient between the elevation of this station (rounded here to 2500 m) and the front of ECH (fixed at 3700 m in this analysis). We do not differentiate solid vs. liquid precipitation because at this glacier (and in other high elevation areas in this portion of the Andes) the bulk of precipitation occurs during the winter months and the fraction of liquid precipitation is usually minimal compared to the large proportion that falls as snow (see Fig. 1D). The use of total precipitation values also avoids the additional complexity and uncertainties involved in differentiating solid from liquid precipitation at this glacier, which is distributed over a very small altitudinal range (see also Fig. 1C). T_i represents mean monthly temperatures at El Yeso extrapolated to the elevation of the glacier front using a constant lapse rate of -0.065°C/100 m, and T_{melt} is the monthly mean temperature above which melt occurs. As indicated in Marzeion et al. (2012), the maximum operator ensures that melting occurs only during months with mean temperatures above T_{melt}. The parameter μ is expressed in mm K^{-1} and was introduced to translate the monthly temperature records into monthly ablation values at the glacier. In order to estimate the parameters α and μ and validate the final model, we performed a "leave-one-out" cross validation procedure (Michaelsen 1987). In this approach, ECH data for each year between 1977 and 2012 (common period between the El Yeso data and the ECH mass balance series) were successively excluded and the minimal mass balance model (Eq. 1) calibrated with the remaining values. At each step the parameters α and μ were first optimized to minimize the root mean squared error (rmse; Weisberg 1985) of the modeled values, and then used to estimate the mass balance data omitted that year. This resulted in 36 predicted values which were compared to the actual annual mass balance observations to compute validation statistics of model accuracy and error. The exercise showed that the model parameters are relatively time stable: α ranged between 3.9 and 4.1 (mean value used here = 3.9), whereas μ varied between 89.0 and 91.0 mm K^{-1} (mean value used = 90.1 mm K^{-1}). The mean estimated value of α indicates that accumulation at the glacier is normally about four times larger than the annual precipitation recorded at El Yeso. The mean estimated value for μ is also reasonable and within the range of values reported by Marzeion et al. (2012) for the 15 glaciers with direct measurements in the European Alps (76-156 mm K^{-1}, see their Table 1). Finally, for the sake of simplicity, we prescribed T_{melt} = 0°C as suggested in Marzeion et al. (2012).

2.3 Glacier mass balance reconstruction

In addition to modeling the interannual mass balance variations of ECH using the temperature and precipitation data from El Yeso, we also used regionally representative hydroclimatic indicators to extend the observed glacier mass balance record prior to 1975. The use of these indicators (regionally-averaged series of winter snow accumulation and mean annual river discharges; see Masiokas et al. 2006) was supported by visual comparisons and correlation analyses which showed strong, statistically significant positive associations not only with the winter record at ECH, but also with the annual mass balance series of this glacier (Table 2 and Fig. 2). The correlation was also positive but weaker between the summer component at ECH and the regional snowpack and streamflow series.

The regionally-averaged record of winter snow accumulation is based on eight selected stations located in the Chilean and Argentinean Andes between 30° and 37°S (Fig. 1A and Table 3). The dataset has been updated from the one used by Masiokas et al. (2012) and contains the longest and most complete snowpack records in this region. Prior to computing the regional average, the individual series were expressed as percentages from their 1981-2010 climatology mean values. A similar approach was used to develop a regional record of mean annual (July-June) streamflow variations. This series was calculated using monthly data from 11 gauging stations with the longest and most complete records in this portion of the Andes (Fig. 1A and Table 3). The resulting snowpack and streamflow composite records cover the 1951-2014 and 1909-2013 periods, respectively (Fig. 2).

The glacier mass balance reconstructions are based on simple linear regression models where the predictand is the 1975-2013 ECH annual mass balance series and the predictors are, alternatively, the regional 1951-2014 snowpack and 1909-2013 streamflow records depicted in Fig. 2. Given the relative shortness of the common period between the predictor and predictand series (39 years), the reconstruction models were also developed using a “leave-one-out” cross-validation procedure (Michaelsen 1987). Here, linear regression models for each year were successively calibrated on the remaining 38 observations and then used to estimate the predictand´s value for the year omitted at each step. A simple linear regression model based on the full calibration dataset (1975-2013) was finally used to reconstruct the mass balance values over the complete period covered by the regional time series. The goodness of fit between observed and predicted mass balance values was tested based on the proportion of variance explained by the regression models and the normality, linear trend, and first- and higher-order autocorrelation of the regression residuals. The uncertainties in each reconstructed mass balance value in year *t* ($\varepsilon_{reco(t)}$) were calculated integrating the standard error of the regression estimate (se_{regr}) and the standard error of the mean annual streamflow values used as predictors in the model ($se_{mean(t)}$). This latter error is derived from the standard deviation of the regional record (σ) and increases as the number of contributing streamflow series (*n*) decreases back in time (see Table 3).

$$\varepsilon_{reco(t)} = \sqrt{se_{regr}{}^2 + se_{mean(t)}{}^2}\text{, with} \qquad (2)$$

$$se_{mean(t)} = \frac{\sigma}{\sqrt{n_{(t)}}} \qquad (3)$$

An independent verification of the reconstructed mass balance records was undertaken by comparing the cumulative patterns of these series with the cumulative mass balances reported for glaciar Piloto Este and for other glaciers with shorter mass balance series available in this portion of the Andes (Fig. 1A and Table 1). We also compared the ECH cumulative series (observed and predicted) with a regional record of glacier advances identified during the 20th century in the Andes between 29° and 35°S. The latter record was compiled in a recent review of glacier fluctuations in extratropical South America and is based on direct observations, reports from documentary evidence, and analyses of aerial photographs and satellite images from this region (see Masiokas et al. 2009). The uncertainty of the cumulative series modeled for ECH ($\varepsilon_{(T)}$) were calculated by propagating (adding) the individual errors estimated for each reconstructed value. That is

$$\varepsilon_{(T)} = \sqrt{\sum_{t=1}^{t=T} \varepsilon_{reco(t)}{}^{2}} \quad (4)$$

3 – Results

3.1. Minimal glacier mass balance model

The 1975-2012 winter and summer values observed at ECH are depicted in Fig. 3A. The winter series shows a long term mean of 2.54 m w.eq. and a larger range of variability (std. dev. 1.24 m w.eq.) than the summer series, which fluctuates around a long term mean of -2.93 m w.eq (std. dev. 0.72 m w.eq.). The observed and modeled annual mass balance series are remarkably similar (Fig. 3B) and show a strong positive correlation (r = 0.883, rmse = 0.77 m w.eq.), indicating that 78% of the variance in the ECH record can be accounted for by the minimal model presented in Eq. (1). Both series show similar, slightly negative linear trends and negative means (-0.35 and -0.34 m w.eq. for the observed and modeled series, respectively) over the 1977-2012 interval.

3.2. Attribution assessments

In order to test which climate variable (temperature or precipitation) has a stronger influence on the annual mass balance variations at ECH, the glacier mass balance model was also run replacing alternatively the temperature and the precipitation monthly data by their long-term average values. The results from this analysis (Fig. 3C) suggest that precipitation variations constitute the dominant forcing modulating annual glacier mass balance at this site. Regardless of their different absolute values, the precipitation-driven estimates (blue dashed line in Fig. 3C) show a strong positive correlation ($r = 0.882$) and remarkable similarities with the ECH annual mass balance series (red line). In contrast, the temperature-driven estimates (dark red dashed line) show a poorer correlation with the ECH record ($r = 0.240$) and a substantially lower inter-annual variability which only barely follows the variations in the annual mass balance series. To evaluate if the influence of temperature had been under-estimated in the full model (where the parameters α and μ can compensate each other), both parameters were also optimized individually using a leave-one-out approach and considering each term of Eq. 1 as separate models. In this case the parameters showed almost exactly the same mean values (3.8 for α and 90.3 mm K^{-1} for μ) as those obtained using the full model (3.9 and 90.1 mm K^{-1} for α and μ, respectively, see section 2.2), suggesting that the poor performance of temperature is not due to the interaction of the parameters in the mass balance model.

3.3 Annual mass balance reconstruction 1909-2013

Fig. 4A shows the reconstruction of the ECH annual mass balance series based on the regional record of mean annual streamflows. The snowpack-based mass balance reconstruction is not shown as it is significantly shorter than the streamflow-based series and shows virtually the same variations over their overlapping interval. The streamflow-based regression model (Table 4) is able to explain 68% of the variance in the annual mass balance series over the 1975-2013 period and shows no apparent sign of model misspecification, offering the possibility of reliably extending the information on glacier mass balance changes back to 1909. This reconstructed mass balance record is almost three times longer than the mass balance record currently available at ECH and shows a strong year-to-year variability embedded within several periods of overall positive or negative conditions (Fig. 4A). In particular, positive mass balance conditions were reconstructed between 1914 and 1941, in the 1980s, and in the late 1990s – early 21st century. In contrast, the clearest sustained period of negative mass balances occurred between the 1940s and the 1970s.

The cumulative values of the streamflow-based mass balance reconstruction show a very good correspondence with the observed cumulative series and an overall negative trend between 1909 and 2013 (Fig. 4B). Within this century-long negative trend, a prominent period of extended positive mass balances can be observed between the mid 1910s and the early 1940s. After 1941 and during the following four decades the cumulative mass balance series shows an impressive decline that is interrupted in 1980 by a ~10-year long period of sustained positive conditions (Fig. 4B). Since the early 1990s and until 2013 the cumulative mass balance series resumes the negative tendency, only interrupted by a short-lived period of positive conditions in the first years of the 21st century. It is important to note, however, that ascribing absolute values to this reconstructed cumulative series is complicated and should be used with caution due to the large uncertainties involved, and the fact that the model is calibrated using reference-surface mass balance estimates (Cogley at al. 2011). Between 1975 and 2013 the lower elevation of the glacier did not change much (see Fig. 1C) and therefore the reference-surface and the conventional mass balance estimates are probably roughly equivalent. However, for earlier decades and without historical information on the glacier area and frontal position, it is difficult to estimate the impacts of changing glacier geometry on the actual mass balance of this glacier.

3.4 Comparison with other glacier records

Examination of the main patterns in the reconstructed cumulative mass balance series shows a good correspondence with a regional record of glacier advances identified in the Central Andes over the past 100 years (Masiokas et al. 2009; Fig. 4C). In most cases, the glacier advances are concentrated during, or soon after, the periods of sustained positive mass balances reconstructed or observed at ECH. This situation is particularly clear in the 1980s and 1990s, where a large number of glacier advances were identified during and/or immediately after the peak in mass balances that culminated in 1989 (Fig. 4BC). Glacier advances were also identified in the 1930s, 1940s and 1950s likely associated with the extended period of cumulative positive mass balances that culminated in the early 1940s. A few well documented advances identified in this region between 2003 and 2007 may be associated with the minor peak in cumulated mass balances observed at the turn of the 21st century (Fig. 4BC).

The cumulative variations in the modeled and observed mass balance series from ECH are also very similar to those observed in the 1979-2002 cumulative record of PIL, providing additional support for the overall reliability of the reconstructed time series (Fig. 5). The cumulative tendency of PIL appears to be “smoother” than the ECH series, but still shows slightly positive or near equilibrium conditions between the late 1970s and the mid 1980s followed by a sharp decline until the turn of the 21st century. The cumulative series from other glaciers located further north in the Pascua Lama and Cordillera de Colanguil areas (Fig. 1A and Table 1) only cover the last decade or so of the ECH record. However, in all cases their overall tendency is similar and markedly negative, reflecting the sustained unfavorable conditions that these ice masses have endured in recent years. It is interesting to note that the smaller glaciers (Table 1 and Fig. 5) are the ones consistently showing the steepest negative cumulative trends whereas the largest glacier (glaciar Guanaco, with ca. 1.8 km^2 in 2007) shows the least negative trend.

4 – Discussion and Conclusions

Compared to other mountainous glacierized areas, the extratropical Andes in southern South America contain one of the least complete networks of *in situ* glacier mass balance and high-elevation climate records in the world. This scarcity of basic information in this extensive and glaciologically diverse region has been highlighted on many occasions, and several recent studies have attempted to overcome this limitation by estimating mass balance changes through remote sensing and/or modeling approaches of varied complexity and spatial coverage (e.g. Casassa et al. 2006; Radić et al. 2013; Lenaerts et al. 2014; Pellicciotti et al. 2014; Schaefer et al. 2013, 2015). With such limited data availability, the few existing glacier mass balance records become particularly relevant as they provide crucial information and validation measures for many glaciological, climatological and hydrological analyses.

In this paper we analyzed an up-to-date compilation of the longest and most complete *in situ* glacier mass balance and hydro-climatic records from the Andes between 29° and 37°S to address some basic (yet poorly known) glaciological issues in this region. First, we show that it is possible to estimate annual glacier mass balance changes using very simple modeling approaches. Results from a minimal model requiring only monthly temperature and precipitation data (eq. 1) revealed that up to 78% of the variance in the annual mass balance series between 1977 and 2012 could be captured simply using available records from the El Yeso station, ca. 10 km from the glacier (Fig. 1A and 3B). Winter precipitation variability appears to be the dominant forcing modulating annual mass balances at ECH, with temperature variations likely playing a secondary role (Fig. 3C). This is particularly interesting because it contrasts with the findings in other regions where the recent glacier behavior is generally more strongly related to changes in temperature instead of precipitation (e.g. Marzeion et al. 2012). However, and although Peña and Narbona (1978) also noted a dominant influence of the winter accumulation term on the resulting annual mass balance of this glacier, the results should be assessed with caution given the simplistic nature of our model and the various factors that ultimately affect the annual mass balance at this site. For example, more detailed assessments should also consider the impact of sublimation on the mass balance of glaciers in this high arid portion of the Andes (McDonell et al. 2013; Pellicciotti et al. 2014).

To test the reliability of the temperature records used to model the glacier mass balance series we correlated the El Yeso monthly temperature record with ERA Interim gridded reanalysis temperatures for the 700 mb geopotential height (roughly 3000 m asl), and also with a 0°C isotherm elevation series available from central Chile (Fig. 6). The El Yeso temperature record shows strong positive correlations with ERA Interim gridded data over an extensive region that includes central Argentina, central Chile and an adjacent area in the Pacific Ocean (Fig. 6A). The El Yeso temperature record also shows clear similarities and a positive significant correlation with the 0°C isotherm elevation series over the 1977-2004 interval (Fig. 6B-C). The independence of these three datasets indicates that the El Yeso mean monthly temperature data are reliable and that the poor performance of this variable in the mass balance modeling exercise is not related to the overall quality of the temperature series. Although this issue is beyond the main purposes of this study, more complex modeling approaches are also needed to evaluate if climate data at higher temporal resolution (instead of monthly values as used here) are capable of capturing a larger percentage of the mass balance variations observed at ECH.

Annual mass balance variations observed at ECH can also be reproduced or estimated accurately through simple linear regression using regionally-averaged winter snowpack or annual streamflow records as predictors (Fig. 4A). This is due to the existence of a strong common hydroclimatic signal in this region, which results in very similar inter-annual variations in winter snow accumulation, mean annual river discharges, and glacier mass balance changes such as those measured at ECH (Fig. 2). This simple approach allows extending the information on glacier mass balance changes several decades prior to the beginning of in situ measurements (back to 1909), and offers the opportunity of putting the existing glacier record in a longer term perspective. Many of the extreme values reconstructed in this study have been documented in historical reports and recent analyses of instrumental hydro-climatic data. For example, the extreme positive values of 1914 and 1919 coincide with extremely wet winters in central Chile (see e.g. Fig. 2; Taulis 1934; Masiokas et al. 2012), whereas the period with above average balances centered in the 1980s or the negative conditions between the 1940s and 1970s have been identified, respectively, as the snowiest and driest intervals during the instrumental era in this region (Masiokas et al. 2010). Examination of the main intra- to multi-decadal patterns in this extended series also indicates that the sustained negative mass balance conditions reported for ECH in recent years are not unusual and were probably surpassed by more negative and longer periods between the 1940s and 1970s (Fig. 4A). However, the impact of a few consecutive years of negative mass balances are more serious today than several decades ago because of the low volume of ice remaining and the poorer overall “health” of the glacier.

The cumulative series of the reconstructed mass balances values (Fig. 4B) shows a steep negative trend that is consistent with the recent loss of ice reported for other glaciers in this region (Fig. 5; Escobar et al. 1995; Rivera et al. 2000; Masiokas et al. 2009). This negative trend has been temporarily interrupted by periods of sustained positive mass balances that, in most cases, precede or coincide with recent glacier re-advances identified at these latitudes in the Andes (Masiokas et al. 2009; Fig. 4C). The clearest example is the relationship between the peak in cumulative mass balances in the mid-late 1980s and the 11 documented glacier advances in the following decade. It is also interesting to note that several of the glacier events that occurred after periods of positive mass balances have been identified as surges (Helbling 1935; Espizua 1986; Masiokas et al. 2009; Pitte et al. 2016). The well-known surges of Grande del Nevado glacier (in the Plomo massif area) in 1933-34, 1984-85, and 2004-2007 are particularly noteworthy as they consistently occurred near the culmination of the three periods with overall positive mass balances in the 1920s-30s, in the 1980s and in the first decade of the 21st century (Fig. 4B). In agreement with the progressively smaller magnitude of these peaks in the cumulative mass balance series, the three Grande del Nevado surges also showed a decreasing power and transferred progressively smaller quantities of mass from the upper to the lower parts of the glacier. Two recent surges of Horcones Inferior glacier in the nearby Mt. Aconcagua area also occurred in the mid 1980s and again between 2002 and 2006, suggesting a possible connection between the development of surging events and the periods with overall positive mass balance conditions in this region (Pitte et al. 2016).

The fact that only limited information is available for ECH together with the use of reference-surface mass balance estimates (see section 2.1) pose interesting yet complicated questions regarding the applicability of this series in related glaciological and/or climatological assessments. Since reference-surface mass balance variations are more closely related to changes in climate than the conventional mass balance of a glacier (Cogley et al. 2011), the reconstructed series discussed here is arguably more relevant to climate-change related studies rather than hydrological studies. If the purpose is to evaluate the hydrological contribution of this ice mass over the last century, then conventional mass balance estimates are necessarily required to take the changing glacier geometry into account. In any case, and considering the relevance of the observed ECH series for regional, hemispheric and global mass balance studies, a reanalysis (Zemp et al. 2013) of the entire mass balance record would probably produce important worthwhile information to properly assess the hydrological impact of the recent ice mass losses in this semi-arid region (e.g. Ragettli et al. 2014). This issue is particularly relevant due to the extended droughts experienced in recent years and the increasing socio-economic conflicts over the limited water resources (almost entirely originating in the mountains) arising on both sides of the Andes.

Keeping these caveats in mind, the common pattern of strongly negative mass balances, the similarities with the few available glacier chronologies, and the regional nature of the predictors used in the ECH reconstruction suggest that this series may nonetheless be considered representative (in relative terms) of the mass balance changes during recent decades in other less studied areas in this region. Reliable data from a larger number of glaciers together with additional studies of the glacier-climate relationships are, however, still needed to support this hypothesis and to identify, for example, the main climatic forcings behind the recent glacier shrinkage observed in the Central Andes of Chile and Argentina (Masiokas et al. 2009). This is a challenging issue due to several factors, including the serious lack of glacier mass balance series and high-elevation climate records, the complex dynamic response of individual glaciers to similar changes in climate, and the great variety of glaciers existing in this region (Pellicciotti et al. 2014). The results discussed in this study offer a useful starting point to address the various pending issues mentioned above and will hopefully stimulate further glaciological, climatological and hydrological research in this poorly known mountainous region.

6 – Acknowledgements

This work was funded by Consejo Nacional de Investigaciones Científicas y Técnicas (CONICET, Argentina), FONDECYT Grant 1121106, and FONDAP Grant 15110009 (Chile). We greatly acknowledge the World Glacier Monitoring Service (http://www.wgms.ch), Dirección General de Aguas (http://www.dga.cl), Dirección Meteorológica de Chile (http://www.meteochile.gob.cl), and Subsecretaría de Recursos Hídricos (http://www.hidricosargentina.gov.ar) for providing the data used in this study. ERA-Interim reanalysis data and correlation maps were provided by the freely available Climate Explorer online application maintained by Geert Jan van Oldenborgh at the Royal Netherlands Meteorological Institute (KNMI; http://climexp.knmi.nl/). E. Berthier acknowledges support from the French Space Agency (CNES) through his TOSCA program, S.U. Nussbaumer acknowledges support from the Swiss National Science Foundation (project PBBEP2-139400), and A. González-Reyes acknowledges the support from CONICYT (Chile) to conduct his PhD studies. The comments and suggestions from the handling Editor and three anonymous reviewers significantly improved the manuscript and are greatly appreciated.

7 – References

Aceituno, P. (1988), On the functioning of the Southern Oscillation in the South American sector. Part I: Surface climate, Mon. Weather Rev., 116, 505– 524.

Casassa, G., Rivera, A. and Schwikowski, M. 2006. Glacier mass-balance data for southern South America (30°S-56°S). In: Glacier Science and Environmental Change (ed P. G. Knight), Blackwell Publishing, Malden, MA, USA. doi: 10.1002/9780470750636.ch47

Cara, L., M. Masiokas, M. Viale, R. Villalba (in press). Assessing snow cover variations in the Río Mendoza upper basin using MODIS satellite imagery. Revista Meteorológica, 25 p. (in Spanish).

Cogley, J.G., R. Hock, L.A. Rasmussen, A.A. Arendt, A. Bauder, R.J. Braithwaite, P. Jansson, G. Kaser, M. Möller, L. Nicholson and M. Zemp, 2011, Glossary of Glacier Mass Balance and Related Terms, IHP-VII Technical Documents in Hydrology No. 86, IACS Contribution No. 2, UNESCO-IHP, Paris.

DGA. 2009. Radio Eco-sondaje en la cuenca del río Maipo y mediciones glaciológicas en el glaciar Tyndall, Campo de Hielo Sur. Dirección General de Aguas, Santiago de Chile, S.I.T. 204, 95 pp.

DGA, 2010. Balance de masa en el glaciar Echaurren Norte temporadas 1997-1998 a 2008-2009. Dirección General de Aguas, Santiago de Chile, 32 pp.

Escobar, F., Casassa G, Pozo V. 1995a. Variaciones de un glaciar de montaña en los Andes de Chile central en las últimas dos décadas. Bull Inst Fr Etud Andin 1995;24(3):683–95.

Escobar, F., Pozo, V., Salazar, A,. y Oyarzo, M., 1995b. Balance de masa en el glaciar Echaurren Norte, 1975 a 1992. Resultados preliminares. Dirección General de Aguas. (Publicación DGA, H.A. y G. 95/1), 106 p.

Escobar, F. and Garín, C. 1997. Complemento Nº 1, años 1993-1996, al “Balance de masa en el glaciar Echaurren Norte, 1975 a 1992. Resultados preliminares”. Dirección General de Aguas. (Publicación DGA, H.A. y G. 97/1), 18 p.

Espizua, L. 1986. Fluctuations of the Río del Plomo Glaciers. Geografiska Annaler, 68A(4): 317-327.

Falvey, M.; Garreaud, R.D. 2009. Regional cooling in a warming world: Recent temperature trends in the southeast Pacific and along the west coast of subtropical South America

(1979–2006). Journal of Geophysical Research 114, D04102, doi:10.1029/2008JD010519.

Garreaud, R.D. 2009. The Andes climate and weather. Advances in Geosciences 7, 1–9.

Helbling, R. 1935. The origin of the Río Plomo ice-dam. The Geographical Journal, 8(1): 41-49.

Kaser, G., Grosshauser, M., and Marzeion, B.: Contribution potential of glaciers to water availability in different climate regimes, P. Natl. Acad. Sci. USA, 107, 20223–20227, doi:10.1073/pnas.1008162107, 2010.

Le Quesne, C., et al. (2009), Long-term glacier variations in the Central Andes of Argentina and Chile, inferred from historical records and tree-ring reconstructed precipitation, Palaeogeogr. Palaeoclimatol. Palaeoecol., 281, 334-344.

Leiva, J.C.; Cabrera, G.A.; Lenzano, L.E. 2007. 20 years of mass balances on the Piloto glacier, Las Cuevas river basin, Mendoza, Argentina. Global and Planetary Change 59, 10–16.

Lenaerts, J.T.M., M.R. van den Broeke, J.M. van Wessem, W.J. van de Berg, E. van Meijgaard, L.H. van Ulft, and M. Schaefer. 2014. Extreme precipitation and climate gradients in Patagonia revealed by high-resolution regional atmospheric climate modeling. Journal of Climate 27, 4607–4621.

Lliboutry, L., 1998: Glaciers of the dry Andes. Satellite Image Atlas of Glaciers of the World: South America, R. S. Williams and J. G. Ferrigno, Eds., USGS Professional Paper 1386-I. Available online at http://pubs.usgs.gov/prof/p1386i/index.html.

MacDonell, S., C. Kinnard, T. Mölg, L. Nicholson, and J. Abermann. 2013. Meteorological drivers of ablation processes on a cold glacier in the semi-arid Andes of Chile. The Cryosphere, 7, 1513–1526, doi:10.5194/tc-7-1513-2013

Marzeion, B., M. Hofer, A. H. Jarosch, G. Kaser, and T. Molg. 2012. A minimal model for reconstructing interannual mass balance variability of glaciers in the European Alps. The Cryosphere, 6, 71–84, doi:10.5194/tc-6-71-2012.

Masiokas, M.H.; Villalba, R.; Luckman, B.; LeQuesne, C.; Aravena, J.C. 2006. Snowpack variations in the central Andes of Argentina and Chile, 1951-2005: Large-scale atmospheric influences and implications for water resources in the region. Journal of Climate 19 (24), 6334-6352.

Masiokas, M.H.; Villalba, R.; Luckman, B.; Delgado, S.; Lascano, M.; Stepanek, P. 2008. 20th-century glacier recession and regional hydroclimatic changes in northwestern Patagonia. Global and Planetary Change 60 (1-2), 85-100.

Masiokas, M.H.; Rivera, A.; Espizua, L.E.; Villalba, R.; Delgado, S.; Aravena, J.C. 2009. Glacier fluctuations in extratropical South America during the past 1000 years. Palaeogeography, Palaeoclimatology, Palaeoecology 281 (3-4), 242-268.

Masiokas, M.H.; Villalba, R.; Luckman, B.H.; Mauget, S. 2010. Intra- to multidecadal variations of snowpack and streamflow records in the Andes of Chile and Argentina between 30° and 37°S. Journal of Hydrometeorology 11 (3), 822-831.

Masiokas, M.H.; Villalba, R.; Christie, D.A.; Betman, E.; Luckman, B.H.; Le Quesne, C.; Prieto, M.R.; Mauget, S. 2012. Snowpack variations since AD 1150 in the Andes of Chile and Argentina (30°-37°S) inferred from rainfall, tree-ring and documentary records. Journal of Geophysical Research - Atmospheres, 117, D05112, doi:10.1029/2011JD016748.

Miller, A., 1976: The climate of Chile. World Survey of Climatology. W. Schwerdtfeger, Ed., Vol. 12, Elsevier, 113–218.

Pellicciotti, F.; Ragettli, S.; Carenzo, M.; McPhee, J. 2014. Changes of glaciers in the Andes of Chile and priorities for future work. Science of the Total Environment 493, 1197–1210.

Peña, H.; Narbona, J. 1978. Proyecto Glaciar Echaurren Norte, Informe preliminar. Dirección General de Aguas, Departamento de Hidrología (in Spanish). 75 p.

Pitte, P.; Berthier, E.; Masiokas, M.H.; Cabot, V.; Ruiz, L.; Ferri Hidalgo, L.; Gargantini, H.; Zalazar, L. 2016. Geometric evolution of the Horcones Inferior Glacier (Mount Aconcagua, Central Andes) during the 2002–2006 surge. Journal of Geophysical Research, Earth Surface, 121, 111–127, doi:10.1002/2015JF003522.

Popovnin, V.V., Danilova, T.A., Petrakov, D.A., 1999. A pioneer mass balance estimate for a Patagonian glacier: Glaciar De los Tres, Argentina. Global and Planetary Change 22 (1), 255–267.

Rabatel, A.; H. Catebrunet, V. Favier, L. Nicholson, C. Kinnard. 2011. Glacier changes in the Pascua Lama region, Chilean Andes (29 S): recent mass balance and 50 years surface area variations. The Cryosphere 5, 1029–1041.

Radić, V.; Bliss, A.; Beedlow, A.C.; Hock, R.; Miles, E.; Cogley, J.G.; Regional and global projections of twenty-first century glacier mass changes in response to climate scenarios from global climate models. Climate Dynamics, DOI 10.1007/s00382-013-1719-7

Ragettli S., Cortés G., McPhee J., Pellicciotti F. 2014. An evaluation of approaches for modelling hydrological processes in high-elevation, glacierized Andean watersheds, Hydrological Processes 28, 5674–5695, doi: 10.1002/hyp.10055

Rignot, E., A. Rivera, G. Cassasa. 2003. Contribution of the Patagonia Icefields to sea level rise. Science 302, 434-437.

Rasmussen, L., Conway, H., Raymond, C., 2007. Influence of upper air conditions on the Patagonia Icefields. Global and Planetary Change 59, 203–216.

Rivera, A., G. Casassa, C. Acuña, and H. Lange, 2000: Recent glacier variations in Chile (in Spanish). Investigaciones Geográficas 34, 29–60.

Rivera, A.; Bown, F; Casassa, G.; Acuña, C.; Clavero, J. 2005. Glacier shrinkage and negative mass balance in the Chilean Lake District (40ºS). Hydrological Sciences Journal, 50(6): 963-974.

Ruiz, L.; Pitte, P.; Masiokas, M. 2013. The initiation of mass balance studies on the Argentinean glaciers on Mount Tronador. CRN2047 Science Meeting, Uspallata, Argentina, April 21-25, 2013.

Schaefer, M., Machguth, H., Falvey, M., Casassa, G. 2013. Modeling past and future surface mass balance of the Northern Patagonia Icefield. J. Geophys. Res., 118, 571–588, doi: 10.1002/jgrf.20038.

Schaefer M., Machguth H., Falvey M., Casassa G., Rignot E. 2015. Quantifying mass balance processes on the Southern Patagonia Icefield. Cryosphere, 9(1), 25–35, doi: 10.5194/tc-9-25-2015.

Taulis, E. 1934. De la distribucion de pluies au Chili. Matér. Étude Calamités, 33, 3-20.

Villalba, R.; Lara, A.; Boninsegna, J.A.; Masiokas, M.H.; Delgado, S.; Aravena, J.C.; Roig, F.; Schmelter, A.; Wolodarsky, A.; Ripalta, A. 2003. Large-scale temperature changes across the southern Andes: 20th-century variations in the context of the past 400 years. Climatic Change 59 (1-2), 177-232.

WGMS. 2013. Glacier Mass Balance Bulletin No. 12 (2010-2011). Zemp, M., Nussbaumer, S.U., Naegeli, K., Gärtner-Roer, I., Paul, F., Hoelzle, M., and Haeberli, W. (eds.), ICSU (WDS)

/ IUGG (IACS) / UNEP / UNESCO / WMO, World Glacier Monitoring Service, Zurich, Switzerland: 106 pp., publication based on database version: doi: 10.5904/wgms-fog-2013-11.

Zemp, M., E. Thibert, M. Huss, D. Stumm, C. Rolstad Denby, C. Nuth, S.U. Nussbaumer, G. Moholdt, A. Mercer, C. Mayer, P. C. Joerg, P. Jansson, B. Hynek, A. Fischer, H. Escher-Vetter, H. Elvehøy, and L. M. Andreassen. 2013. Reanalysing glacier mass balance measurement series. The Cryosphere, 7, 1227–1245, doi:10.5194/tc-7-1227-2013

Table 1. Basic information of the glacier mass balance series used in this study. (*) Country: CL: Chile; AR: Argentina.

Name	ID in Fig. 1	Lat., Long.	Area in km^2 (year)	Period	Ctry*	References
Echaurren Norte	ECH	33°33’S, 70°08’W	0.226 (2008)	1975-2013	CL	DGA 2009; Barcaza (DGA); WGMS 2013
Piloto Este	PIL	32°13’S, 70°03’W	0.504 (2007)	1979-2002	AR	Leiva et al. 2007; WGMS 2013
Conconta Norte	COL	29°58’S, 69°39’W	0.089 (2012)	2008-2013	AR	Cabrera and Leiva (IANIGLA); WGMS 2013
Brown Superior	COL	29°59’S, 69°38’W	0.191 (2012)	2008-2013	AR	Cabrera and Leiva (IANIGLA); WGMS 2013
Los Amarillos	COL	29°18’S, 69°59’W	0.954 (2012)	2008-2013	AR	Cabrera and Leiva (IANIGLA); WGMS 2013
Amarillo	PAS	29°18’S, 70°00’W	0.243 (2012)	2008-2013	CL	Cabrera and Leiva (IANIGLA); WGMS 2013
Toro 1	PAS	29°20’S, 70°01’W	0.071 (2007)	2004-2009	CL	Rabatel et al. 2011; WGMS 2013
Toro 2	PAS	29°20’S, 70°01’W	0.066 (2007)	2004-2009	CL	Rabatel et al. 2011; WGMS 2013
Esperanza	PAS	29°20’S, 70°02’W	0.041 (2007)	2004-2009	CL	Rabatel et al. 2011; WGMS 2013
Guanaco	PAS	29°19’S, 70°00’W	1.836 (2007)	2004-2013	CL/ AR	Rabatel et al. 2011; Rivera (CECs); WGMS 2013

Table 2. Correlation analyses between the ECH mass balance series and regional hydro-climatic records. The number of observations used in each correlation test is indicated in parenthesis. Note: * (**) Pearson correlation coefficient is significant at the 95% (99%) confidence level.

	Winter ECH	Annual mass balance ECH	Regional snowpack	Regional streamflow
Summer ECH	0.245 (38)	0.648** (38)	0.447** (38)	0.395* (38)
Winter ECH		0.897** (38)	0.796** (38)	0.834** (38)
Annual mass balance ECH			0.829** (39)	0.826** (39)
Regional snowpack				0.916** (63)

Table 3. Stations used to develop regionally-averaged series of mean annual river discharges and winter maximum snow accumulation for the Andes between 30° and 37°S. Mean annual streamflow values refer to a July-June water year. Note: (*) The 1981-2010 climatology values for each station are expressed as mm w.eq. for snowpack and as $m^3 s^{-1}$ for streamflow. In the case of the San Juan and Cachapoal rivers, the mean values used correspond to the 1981-2007 and 1981-2001 periods, respectively. Data sources: (DGA) Dirección General de Aguas, Chile; (DGI) Departamento General de Irrigación, Mendoza, Argentina; (SSRH) Subsecretaría de Recursos Hídricos, Argentina. See Masiokas et al. (2013) for further details.

Variable	**Station**	**Lat., Long.**	**Elev.**	**Period**	**1981-2010 mean***	**Data source**
A - Snowpack	Quebrada Larga	30°43'S, 70°22'W	3500 m	1956-2014	273	DGA
	Portillo	32°50'S, 70°07'W	3000 m	1951-2014	703	DGA
	Toscas	33°10'S, 69°53'W	3000 m	1951-2014	354	DGI
	Laguna Negra	33°40'S, 70°08'W	2768 m	1965-2014	632	DGA
	Laguna del Diamante	34°15'S, 69°42'W	3310 m	1956-2014	472	DGI
	Valle Hermoso	35°09'S, 70°12'W	2275 m	1952-2014	756	DGI
	Lo Aguirre	36°00'S, 70°34'W	2000 m	1954-2014	934	DGA
	Volcán Chillán	36°50'S, 71°25'W	2400 m	1966-2014	757	DGA
B - Streamflow (river)	Km. 47.3 (San Juan)	31°32'S 68°53'W	945 m	1909- 2007	68.2	SSRH
	Guido (Mendoza)	32°51'S 69°16'W	1550 m	1909-2013	52.4	SSRH
	Valle de Uco (Tunuyán)	33°47'S 69°15'W	1200 m	1954-2013	30.6	SSRH
	La Jaula (Diamante)	34°40'S 69°19'W	1500 m	1938-2013	35.6	SSRH
	La Angostura (Atuel)	35°06'S 68°52'W	1200 m	1948-2013	39.1	SSRH
	Buta Ranquil (Colorado)	37°05'S 69°44'W	850 m	1940-2013	154.8	SSRH
	Cuncumén (Choapa)	31°58'S 70°35'W	955 m	1941-2013	10.3	DGA
	Chacabuquito (Aconcagua)	32°51'S 70°31'W	1030 m	1914-2013	34.7	DGA
	El Manzano (Maipo)	33°36'S 70°23'W	890 m	1947-2013	123.0	DGA
	Termas de Cauquenes (Cachapoal)	34°15'S 70°34'W	700 m	1941-2001	93.6	DGA
	Bajo Los Briones (Tinguiririca)	34°43'S 70°49'W	518 m	1942-2013	53.8	DGA

Table 4. Summary statistics for the simple linear regression models used to estimate ECH annual mass balances using regional snowpack and streamflow records. Notes: (adj r^2) adjusted coefficient of determination used to estimate the proportion of variance explained by regression; (F) F-ratio for ANOVA test of the null hypothesis that all model coefficients are 0; (Se) standard error of the estimate; (rmse) root-mean-squared error of regression. (b0) constant of regression model; (b1) regression coefficient; (DWd) Durbin-Watson d statistic used to test for first-order autocorrelation of the regression residuals. (Port. Q) Portmanteau Q statistic to test if high-order autocorrelation in the regression residuals is different from 0. (ns) results are not statistically significant at the 95% confidence level; (**) statistically significant at the 99% confidence level.

Predictor	**Model statistics**						**Residual statistics**		
	Adj r^2	F	Se	rmse	b0 (std. error)	b1 (std. error)	Slope	DWd	Port. Q
Snowpack	0.686	80.99**	0.889	0.911	-2.899 (0.316)**	0.026 (0.003)**	-0.003ns	2.2ns	5.7ns
Streamflow	0.682	79.49**	0.894	0.919	-4.045 (0.439)**	0.038 (0.004)**	0.006ns	2.3ns	4.9ns

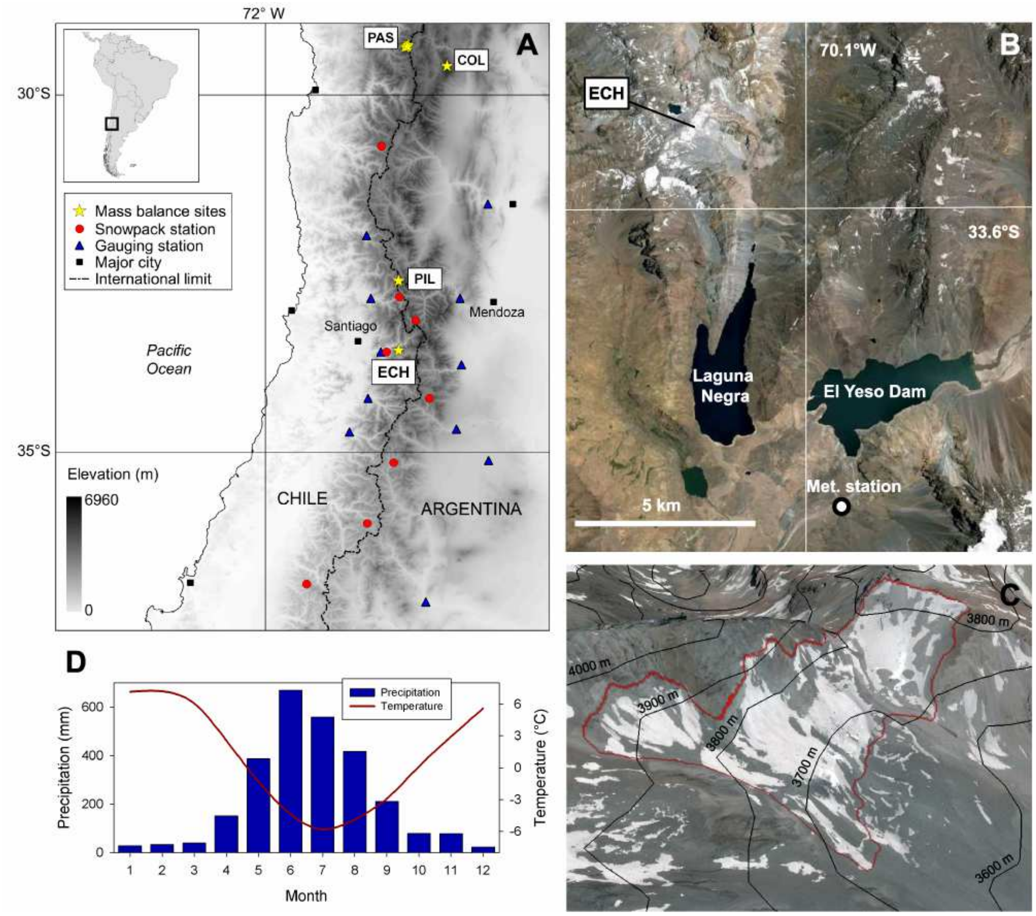

Figure 1. A) Map of the Central Andes of Chile and Argentina showing the location of glaciar Echaurren Norte (ECH), glaciar Piloto Este (PIL), and several smaller glaciers with mass balance records in the Pascua Lama (PAS) and Cordillera de Colanguil (COL) areas. The locations of the snowpack and streamflow stations discussed in the text are also shown (Tables 1 and 2). **B)** General view of the El Yeso area, showing the location of ECH, El Yeso Dam, and the associated meteorological station. Laguna Negra is a natural lake that receives the meltwater from ECH. Base image acquired on January 5, 2014 and downloaded from Google Earth. **C)** Closer 3D view of glaciar Echaurren Norte as observed in 2014 and in the early 1970s (outlined in red and based on Peña and Narbona 1978). Note that the glacier has remained in roughly the same position but has thinned markedly over the last decades. **D)** Seasonal variations in temperature and precipitation at the lower reaches of ECH (3700 m asl) extrapolated from the El Yeso meteorological station (see section 2.2 for details). Note that the bulk of precipitation occurs during the coldest months of the year (December-March precipitation only accounts for ~5% of the mean annual totals).

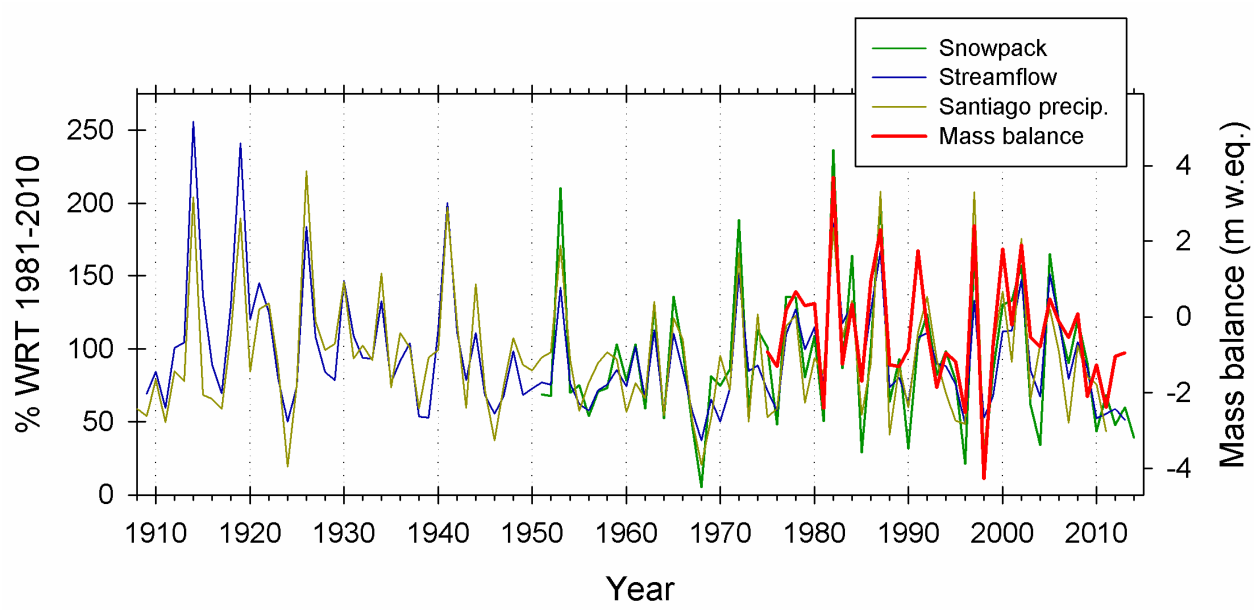

Figure 2. Comparison between the annual mass balance series of ECH and regional records of maximum winter snow accumulation and mean annual river discharges in the Andes between 30° and 37°S (see Fig. 1). The regional records are expressed as percentages with respect to the 1981-2010 mean values. Variations in annual total precipitation at Santiago are also included to highlight the strong hydro-climatic signal in this region.

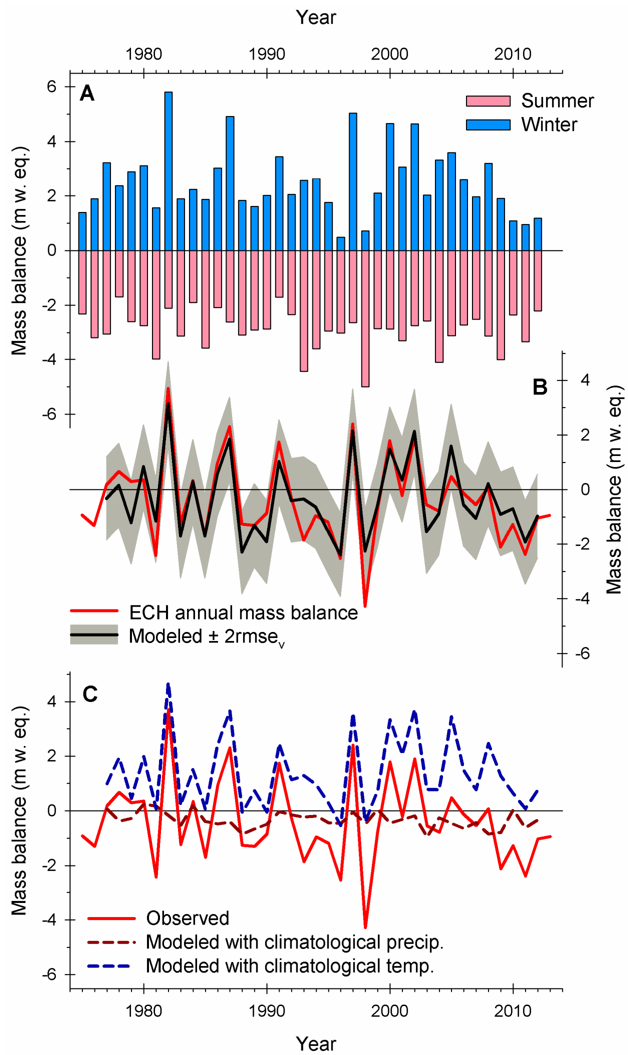

Figure 3. (A) Winter and summer values observed at ECH between 1975 and 2012. **(B)** Annual mass balance series observed at ECH and modeled using El Yeso climate data (red and black lines, respectively). The estimated uncertainties of the modeled values (± 2 rmse) are shown with gray shading. **(C)** Annual mass balances observed at ECH (red line) compared to mass balances modeled using full variability in temperature but climatological monthly precipitation (dark red dashed line), and full variability in precipitation but climatological monthly temperatures (dark blue dashed line). Note the greater similarities between the observed series and the precipitation-based mass balance estimates.

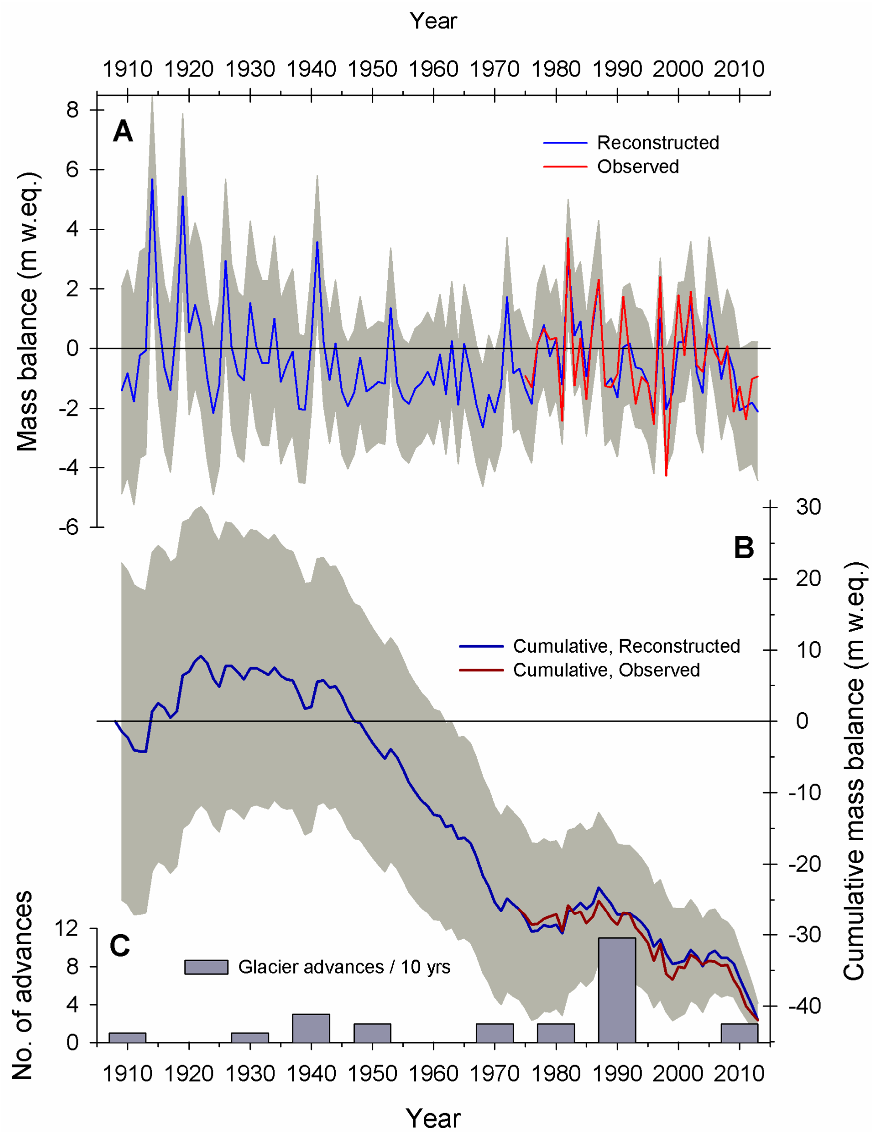

Figure 4. (A) Comparison between the annual mass balance record observed at ECH (red line) and the reconstructed series derived from regionally-averaged streamflow data (blue line). The estimated uncertainty of the reconstructed series (±2 ε_{reco}) is indicated by gray shading. **(B)** Cumulative record of the observed and reconstructed ECH mass balance series (dark red and dark blue lines, respectively). The initial value of the observed ECH cumulative record was modified to match the corresponding value in the reconstructed series. The aggregated errors in this series (see section 2.3) are also shown by gray shading **(C)** Glacier advances identified in the central Andes of Chile and Argentina during the past 100 years (see text for details). Events are grouped into 10-year intervals.

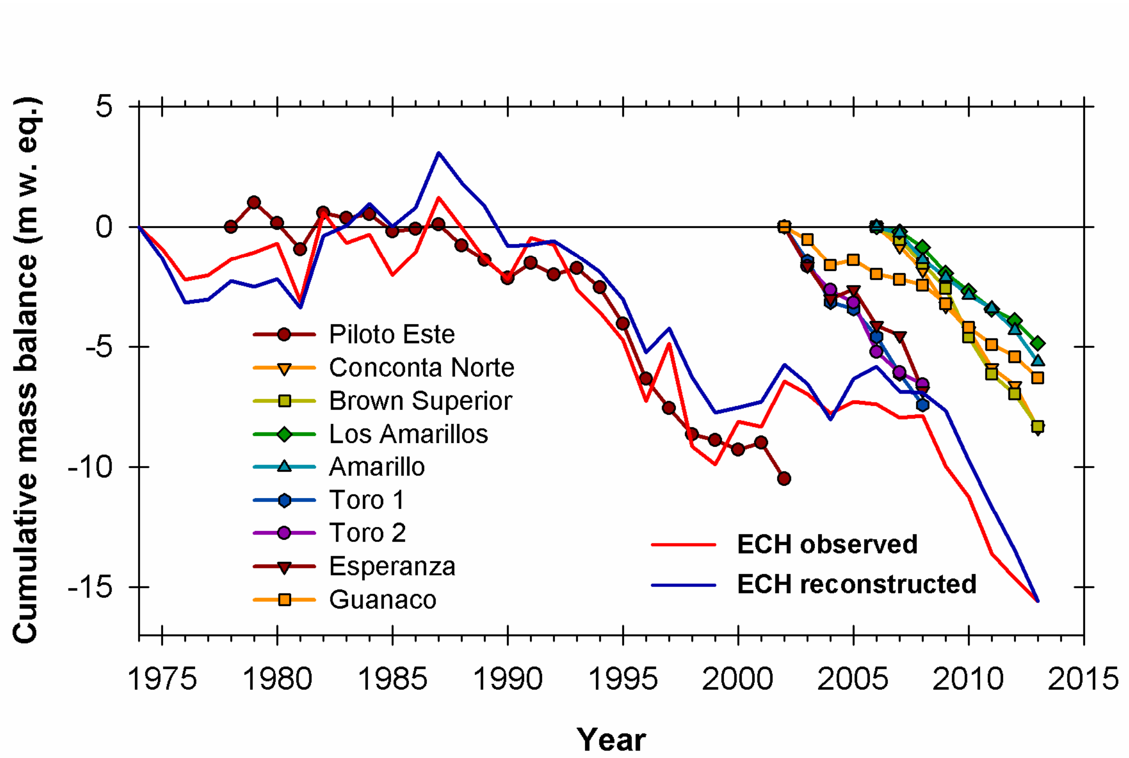

Figure 5. Comparison between the cumulative patterns in the observed and reconstructed records from ECH and other glaciers with available direct mass balance data in the Dry Andes of Chile and Argentina (Fig. 1 and Table 1).

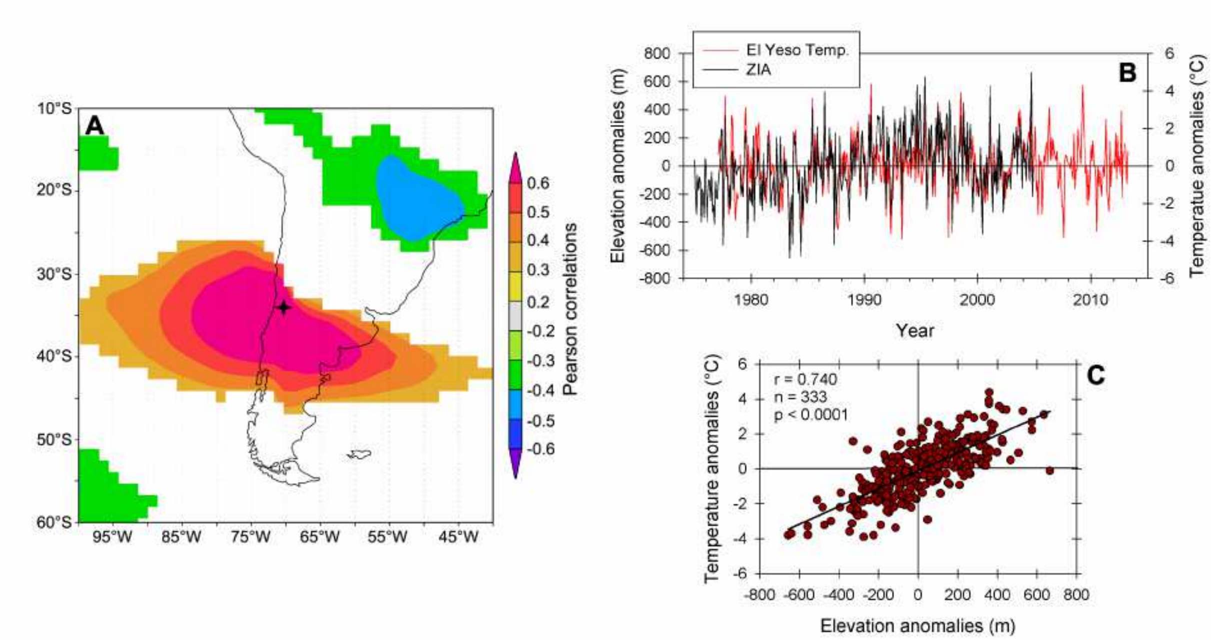

Figure 6. A) Map showing the correlations (p<0.1) between mean warm season (October-March) temperatures at the El Yeso station and gridded warm season ERA Interim mean temperatures for the 700 mb geopotential height level over the 1979-2012 period. The black star marks the location of the El Yeso station. **B)** Diagram showing variations of mean monthly temperatures at El Yeso (1977-2013) and the mean monthly elevation of the 0°C isotherm (ZIA) derived from radiosonde data from the Quintero coastal station (1975-2004). To facilitate the comparison, both series are expressed as anomalies from their mean seasonal cycles. **C)** Scatterplot of the El Yeso temperature and ZIA anomalies depicted in B. Note the positive, highly significant correlation between these two variables. ZIA data were provided by J. Carrasco from Dirección Meteorológica de Chile.